NATIONAL ADVISORY COMMITTEE FOR AERONAUTICS

TECHNICAL NOTE

No. 1244

EFFECT OF THE TUNNEL-WALL BOUNDARY LAYER ON TEST RESULTS OF A WING PROTRUDING FROM A TUNNEL WALL

By Robert A. Mendelsohn and Josephine F. Polhamus

Langley Memorial Aeronautical Laboratory
Langley Field, Va.

Washington

April 1947

NATIONAL ADVISORY COMMITTEE FOR AERONAUTICS

TECHNICAL NOTE NO. 1244

EFFECT OF THE TUNNEL-WALL BOUNDARY LAYER ON TEST RESULTS OF A WING PROTRUDING FROM A TUNNEL WALL

By Robert A. Mendelsohn and Josephine F. Polhamus

SUMMARY

Two-dimensional span-loading tests were made of a two-foot-chord NACA 65_1-012 airfoil model in the $2\frac{1}{2}$-foot by 6-foot test section of the Langley stability tunnel to determine tunnel-wall boundary-layer effects. The tests indicated that a small loss (less than one percent of the load at the center) in average load may be expected. At the tunnel wall the load may be as much as 10 percent lower than that at the center of the tunnel, and large changes in the tunnel-wall boundary-layer thickness produce small changes in load. At low angles of attack the tunnel-wall boundary layer had little effect on the pitching moment. At high angles of attack, the average pitching moment for the wing may differ from the pitching moment at the center of the tunnel because of nonuniform stall.

INTRODUCTION

A large amount of work is being done with models that completely span the tunnel test section and with semispan models that use the tunnel wall as a reflection plane. Because of the possibility that the tunnel-wall boundary layer affects the flow near the walls and thus alters the airfoil characteristics in this region, it would be desirable to have some knowledge of the magnitudes of the effects and to find possible ways of correcting for them.

Estimation of tunnel-wall boundary-layer effects on a two-dimensional model is based in reference 1 on the assumption that the loading on the model will be decreased at each end in proportion to the square of the local velocity through the tunnel-wall boundary layer. Reference 1 also assumes that this change in loading will produce induced effects over the whole model and will cause an appreciable error in measured results for most ratios of model chord

to model span. From computations of the vortex strength in terms of tunnel-wall boundary-layer thickness, an estimate of the induced angle-of-attack loading over the wing is made by a consideration of tunnel width and model chord. Large changes in loading are shown to be possible from these calculations, and it is suggested that, for two-dimensional tests, the model be mounted between a pair of dummy ends that are shaped to the model contour and fastened to the tunnel wall.

In most cases, the practice of the NACA for two-dimensional tests of models completely spanning the test section is to neglect any correction for tunnel-wall boundary-layer effects. Instead of mounting the model on balances, several NACA tunnels determine model lift by pressure integration over a section of the tunnel walls, and this method of determining lift minimizes the error caused by the tunnel-wall boundary layer.

The tests herein described were run for the purpose of verifying experimentally the supposition that although there would be a velocity gradient through the boundary layer, it would be caused by a local change in total pressure and that the static pressure, and consequently the airfoil lift, would remain essentially constant across the model span. A quantitative determination of the change in model loading near a tunnel wall was also considered valuable for evaluating the accuracy with which semispan-model tests approximate full-span model tests.

The pressure distribution about a two-dimensional wing was determined for various angles of attack and for various distances from a tunnel wall. These measurements were made for both an erect- and an inverted-model condition, and a mean was taken of integrated forces and moments in order to eliminate possible errors caused by local changes in tunnel stream angle. Tests were run with a normal tunnel-wall boundary layer and with a tunnel-wall boundary layer thickened by means of spoilers on the tunnel wall.

SYMBOLS

The coefficients and symbols used in this report are defined as follows:

c_l section lift coefficient

$c_{l_{max}}$ maximum spanwise section lift coefficient for a given angle of attack

$c_{m_{c/4}}$ quarter-chord pitching-moment coefficient

c airfoil chord

P pressure coefficient $\left(\frac{p - p_o}{q}\right)$

p local static pressure

p_o free-stream static pressure

q dynamic pressure

u local velocity in the boundary layer

U velocity at edge of boundary layer

b tunnel width (30 inches)

x distance from leading edge of wing along chord line

y spanwise distance from tunnel wall

z vertical distance above airfoil surface

α angle of attack

APPARATUS AND METHODS

Model.- A two-foot-chord model of NACA 65_1-012 airfoil section was mounted between the walls of the $2\frac{1}{2}$-foot by 6-foot test section of the Langley stability tunnel in such a manner that the model center section containing the pressure orifices could be located at various distances from the tunnel wall by sliding the wing laterally. The model was six feet in length and was sealed at the tunnel-wall juncture by felt pads clamped firmly against the surface. Changes in angle of attack were accomplished by rotation of tunnel-wall end disks into which the model fitted. (See figs. 1 and 2.)

Although the model was equipped with a true-contour 0.20c plain flap, the flap was in a neutral position for all tests. The airfoil contour at the flap gap was faired by means of "Scotch" cellulose tape.

Tests.- Pressure distributions about a section of the wing for angles of attack of 3.1° and 12.3° were determined for a number of

spanwise locations from the tunnel wall. In addition, a more complete range of angle of attack was used for the tunnel-center orifice location. The dynamic pressure was changed from 40 pounds per square foot at high angles of attack to 100 pounds per square foot at low angles of attack in order to obtain large pressure readings for better accuracy. These dynamic pressures correspond to Reynolds numbers of 2.32×10^6 and 3.66×10^6, respectively. In order to eliminate possible errors caused by a spanwise variation in tunnel stream angle, tests were made with the model both erect and inverted, and a mean of the two tests taken. Because a low-drag airfoil was used, and it was possible that a change in loading would be caused by a nonuniform position of transition, some tests were made with a transition tape at the leading edge of the model. In order to check the effects of the felt seal, tests were made with a modeling-clay seal at the tunnel wall.

Tests were made for three conditions of tunnel-wall boundary layer, as obtained by the use of narrow wire screens attached to the tunnel wall at the entrance cone. These screens extended from ceiling to floor and were pivoted at a point close to the tunnel wall in order to obtain changes in deflection. The outer edge of the screen was deflected 2 inches for spoiler 1 and 3 inches for spoiler 2. Tests were also made with no spoiler.

Corrections.- Tunnel-wall corrections were applied to the angle of attack, the lift coefficient, and the pitching-moment coefficient. (See reference 2.) No tunnel-wall corrections were applied to the pressure distributions or the boundary-layer data. The equations used in correcting the data are:

$$\alpha = 1.0229\alpha_U$$

$$c_l = 0.9671c_{l_U}$$

$$c_{m_{c/4}} = 0.99\left(c_{m_{c/4}}\right)_U + 0.0057c_{l_U}$$

where the subscript U designates uncorrected values. Corrections were applied to the survey-rake tube heights for effective center location in a total-head pressure gradient as outlined in reference 3.

RESULTS AND DISCUSSION

Tunnel-wall velocity profiles.- Figure 3 presents the profiles of the velocity through the tunnel-wall boundary layer for a position six inches ahead of the location of the model leading edge for the

conditions with no tunnel-wall spoiler, with spoiler 1, and with spoiler 2. With no spoiler, the tunnel-wall boundary layer is considerably smaller in this tunnel than in most tunnels of this size because of the high contraction ratio and relatively short distance from entrance cone to test section. The tunnel-wall boundary-layer thicknesses corresponding to the three spoiler deflections probably include most of the tunnel-wall boundary-layer conditions likely to be encountered in practice.

Pressure distributions.- For the condition with spoiler 2, section pressure distributions at $\alpha = 3.1^\circ$ and $\alpha = 12.3^\circ$ for an erect- and an inverted-model configuration and for several spanwise tunnel positions are presented in figure 4. The tests indicate a higher loading with the model inverted than with the model erect. This result may be caused by misalinement of the wing template, by a tunnel stream angle, by a small flap deflection, or by any combination of these effects. Since a mean of the erect and inverted tests was taken for the span-loading and pitching-moment results, most of these effects are averaged out.

At $\alpha = 3.1^\circ$ with spoiler 2, figure 4(a) shows that the peak pressure on the upper surface decreases in magnitude as the tunnel-wall position is approached. At $\alpha = 12.3^\circ$ (fig. 4(b)) no definite decrease through the tunnel-wall boundary layer is shown. The flat peaks on the pressure distributions indicate that, for $\alpha = 12.3^\circ$, extensive regions of laminar separation exist near the leading edge of the upper surface for spanwise positions outside of the boundary layer. The large adverse pressure gradient necessary to cause the laminar separation was not in all cases measured by the static-pressure orifices, and consequently the curves are shown dotted. Within the boundary layer, the magnitude of the flat regions becomes smaller because of turbulent mixing. Because of the change in total pressure through the boundary layer, full free-stream stagnation pressure was not reached by any of the pressure orifices.

Figure 5 presents a comparison of pressure distributions for no tunnel-wall spoiler and for spoiler 2. Because of the smaller tunnel-wall boundary layer for the no-tunnel-wall spoiler condition, a closer approach to stagnation pressure is reached for the stations close to the tunnel wall. (See fig. 5(b).) In general, no large consistent differences in pressure distribution are shown by increasing the boundary-layer thickness.

Spanwise surveys.- Figure 6 illustrates the method used in averaging test results. From a faired curve for erect-model results and a faired curve for inverted-model results an average curve was drawn. The ordinate values of this average curve were then divided by the maximum value, and the resulting parameter $c_l/c_{l_{max}}$ is shown

plotted in figure 7. This maximum value was used in place of the value corresponding to a tunnel having no wall boundary layer because an estimate of the load-loss induced effects showed that at the center of the tunnel the effect was negligible. Figure 7 presents nondimensional span-loading curves for angles of attack of 3.1° and 12.3° and for three conditions of the tunnel-wall boundary layer. In addition, a theoretical curve computed by the methods of reference 1 is presented. This curve represents results for a model that was assumed to operate at unit lift coefficient before taking into account the reduction in loading corresponding to the spoiler 2 condition. It appears that the theory of reference 1 strongly over-estimates the effect of the boundary layer. Although for the model investigated a small loss in average load occurs in the region of the tunnel wall for all spoiler conditions, the loss is small enough (less than one percent of load at center) to be neglected in most force tests. For pressure investigations on semispan models such as span loading or internal-balance pressure measurements, however, local errors as high as 10 percent may result at the tunnel wall. As a check on the possibility that the felt seals were leaking, repeat tests at $\alpha = 3.1°$ were run with modeling clay to form a seal at the tunnel wall. Figure 7 shows that little change occurred. Transition tapes placed at the leading edge to simulate a rough-model condition produced a small loss in average load. For $\alpha = 12.3°$, the load is shown to decrease near the center of the tunnel because of nonuniform stall characteristics.

Curves of section quarter-chord pitching-moment coefficient for the same test conditions as those of figure 7 are presented in figure 8. The spanwise change in pitching moment is negligible for $\alpha = 3.1°$. For $\alpha = 12.3°$, because of the nonuniform stall characteristics, a spanwise change in pitching moment is noted. Flap section hinge-moment coefficients were determined for a simulated 0.20c plain flap by integration of the pressure distributions for the region from the hinge line to the trailing edge. These results indicated that for an angle of attack of 3.1°, the spanwise variation of flap section hinge-moment coefficient was just as great outside the tunnel-wall boundary layer as inside. At an angle of attack of 12.3°, the flap section hinge-moment coefficient became slightly more positive in the region of the tunnel wall.

Force and moment coefficients.- Figure 9 presents the variation of lift coefficient and quarter-chord pitching-moment coefficient with angle of attack as averaged from pressure distributions measured in the center of the tunnel for both erect- and inverted-model configurations. Indicated on the curves are the average values for the complete span. These values represent the results which would be obtained if the model were fastened to balances. For angles of attack of both 3.1° and 12.3°, the balance lift-coefficient estimates

checked very well with the tunnel-center results. At an angle of attack of 3.1°, the difference was very small in terms of the lift coefficient and at an angle of attack of 12.3°, because of nonuniform span loading caused by stalled flow, the close check indicated by figure 9 is probably accidental. The average pitching moment for the wing was slightly more negative than the tunnel-center value at an angle of attack of 3.1° but at an angle of attack of 12.3° the average value over the span was less negative than the tunnel-center value because of nonuniform stall.

CONCLUDING REMARKS

Tests of a two-foot-chord model in the $2\frac{1}{2}$-foot by 6-foot test section of the Langley stability tunnel to determine tunnel-wall boundary-layer effects on wings protruding from a tunnel wall show that a small loss in average load may be expected (less than one percent of load at center). At stations very close to the wall, the local load may be as much as 10 percent lower than that at the center of the tunnel, and large changes in the tunnel-wall boundary-layer thickness produce small changes in load. Also, at low angles of attack a tunnel-wall boundary layer has little effect on the pitching moment. At high angles of attack the average pitching moment for the wing may be different from the value at the center of the tunnel because of nonuniform stall.

Langley Memorial Aeronautical Laboratory
National Advisory Committee for Aeronautics
Langley Field, Va. January 2, 1947

REFERENCES

1. Preston, J. H.: The Interference on a Wing Spanning a Closed Tunnel, Arising from the Boundary Layers on the Side Walls, with Special Reference to the Design of Two-Dimensional Tunnels. R & M No. 1924, British A.R.C., 1944.

2. Allen, H. Julian, and Vincenti, Walter G.: Wall Interference in a Two-Dimensional-Flow Wind Tunnel with Consideration of the Effect of Compressibility. NACA ARR No. 4K03, 1944.

3. Young, A. D., and Maas, J. N.: The Behaviour of a Pitot Tube in a Transverse Total-Pressure Gradient. R. & M. No. 1770, British A.R.C., 1937.

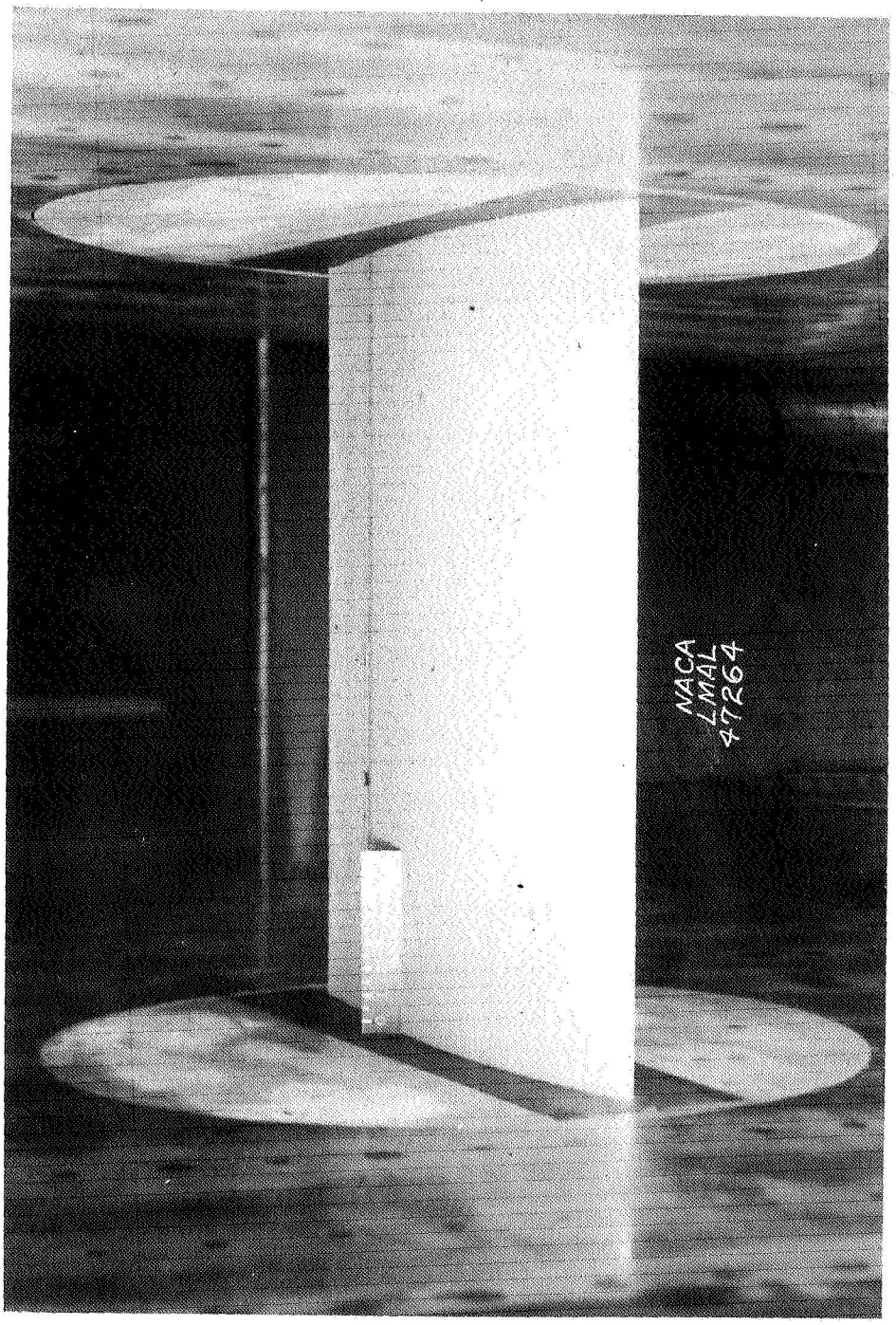

(a) Front view.

Figure 1.- View of the NACA 65_1-012 airfoil model in $2\frac{1}{2}$- by 6-foot test section of Langley stability tunnel.

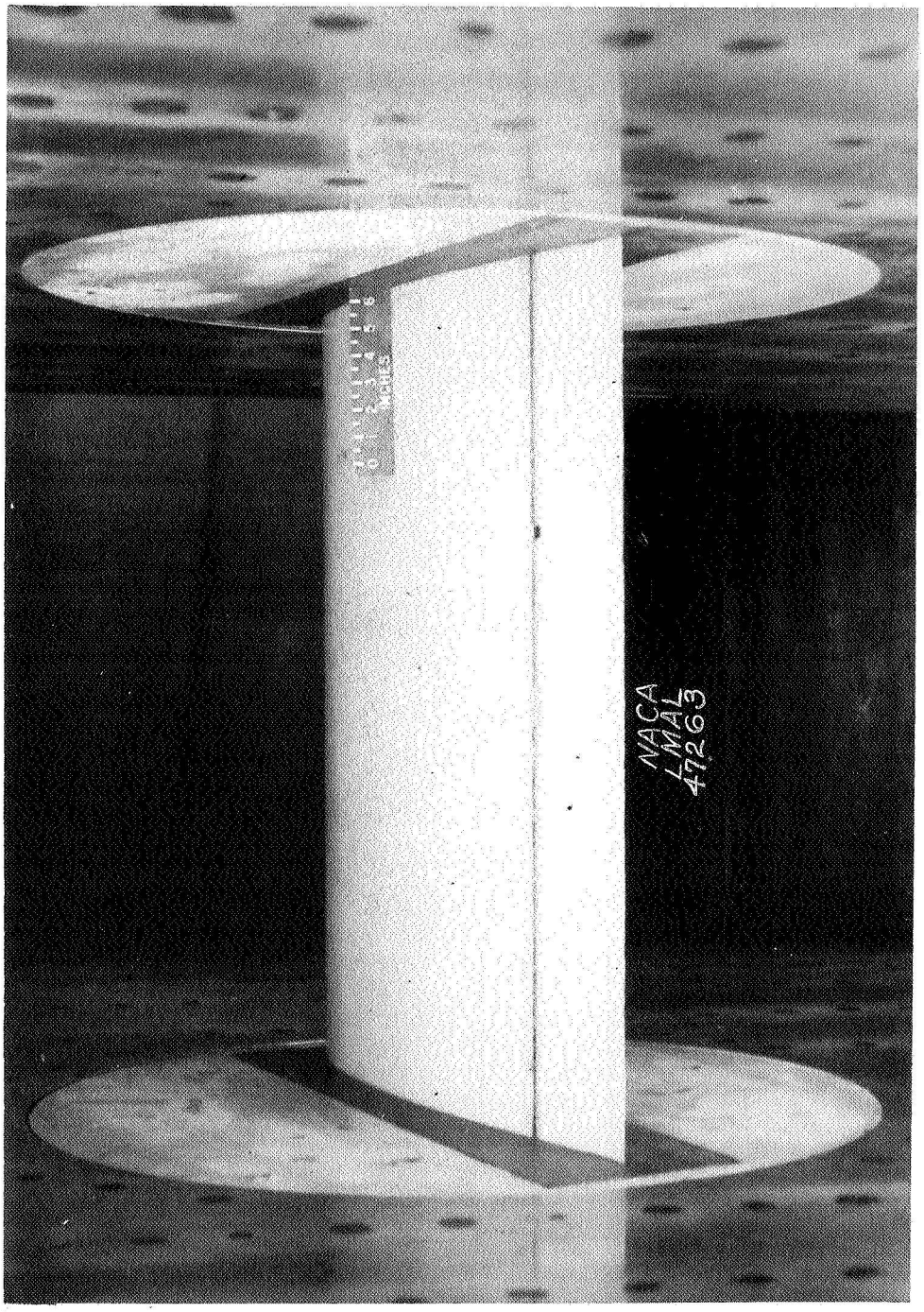

(b) Rear view.

Figure 1.- Concluded.

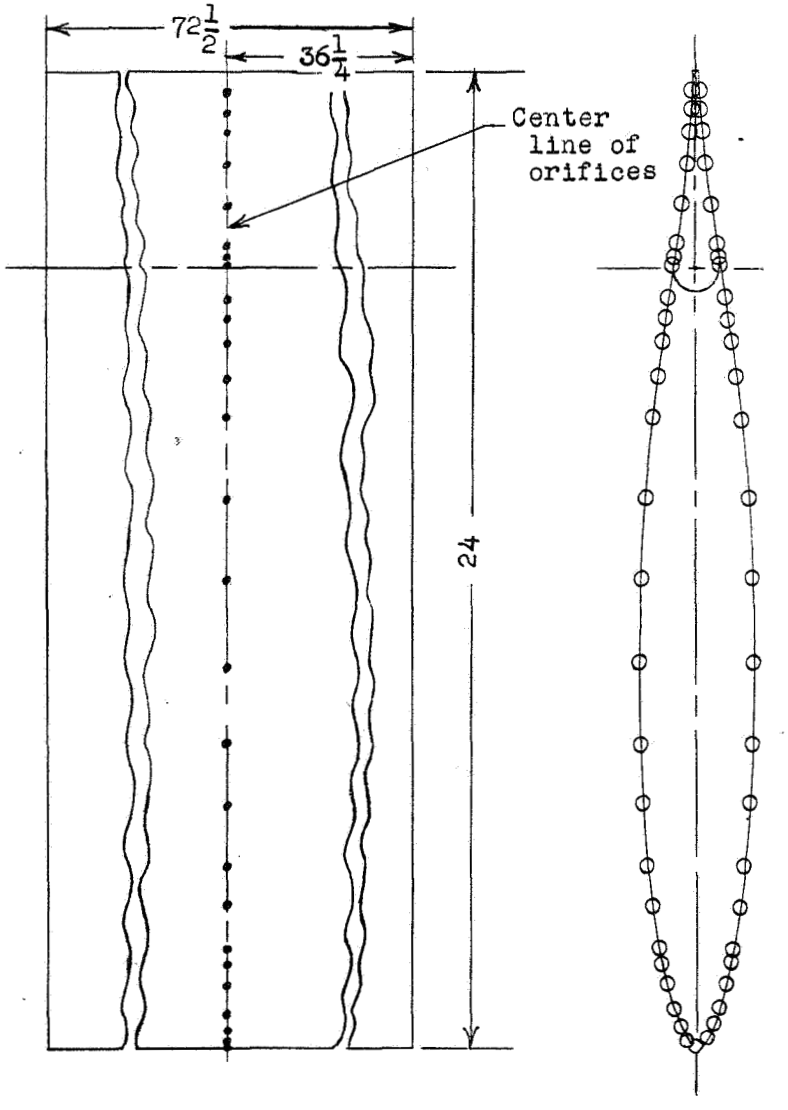

Airfoil ordinates (percent chord)		Orifice locations (percent chord)
Station	Ordinate	Station
0	0	0
.5	.923	.50
.75	1.109	1.5
1.25	1.387	3.5
2.5	1.875	6.0
5.0	2.606	8.0
7.5	3.172	10.0
10.0	3.647	14.5
15.0	4.402	18.5
20.0	4.975	25.0
25.0	5.406	31.0
30.0	5.716	39.5
35.0	5.912	47.9
40.0	5.997	56.0
45.0	5.949	64.6
50.0	5.757	68.4
55.0	5.412	72.1
60.0	4.943	74.6
65.0	4.381	76.7
70.0	3.743	80.0
75.0	3.059	80.8
80.0	2.345	82.3
85.0	1.630	86.3
90.0	.947	90.6
95.0	.356	93.8
100.0	0	95.8
		97.9
L.E. radius: 1.000 percent c		

NATIONAL ADVISORY
COMMITTEE FOR AERONAUTICS

Figure 2.- Dimensions and pressure-orifice locations for the NACA 65_1-012 airfoil.

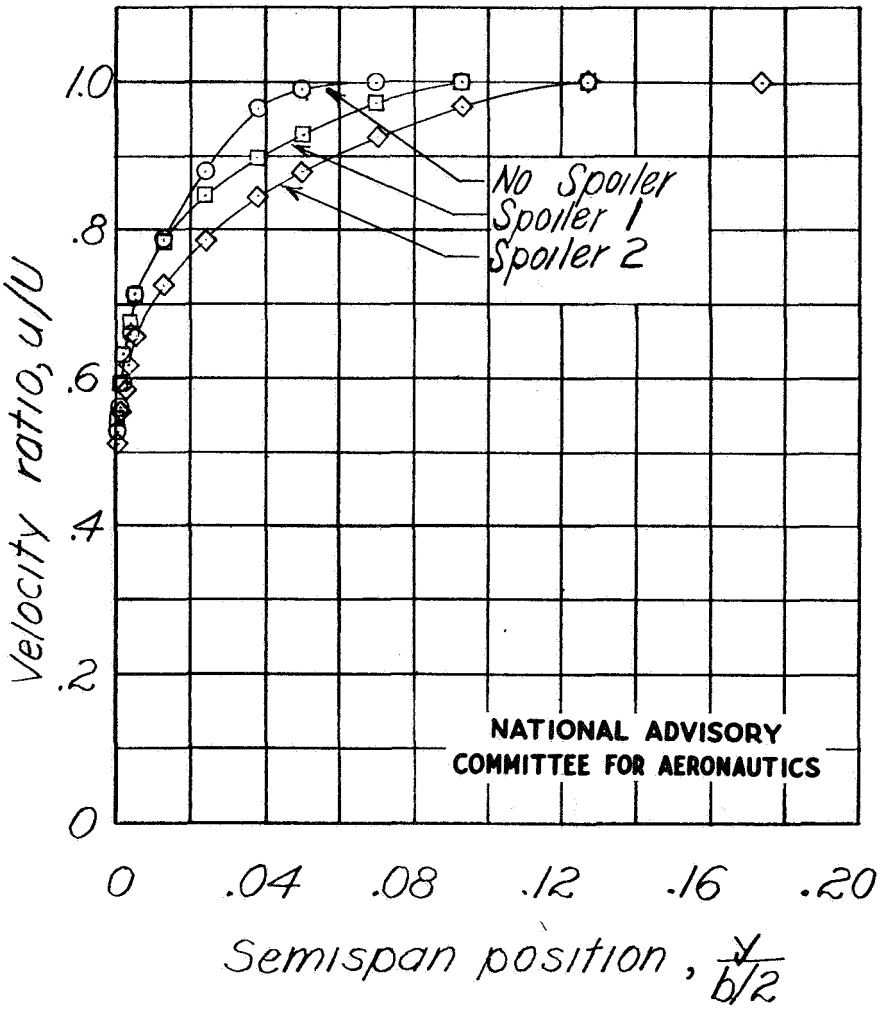

Figure 3.- Tunnel-wall boundary layer for various spoiler conditions. No model in tunnel.

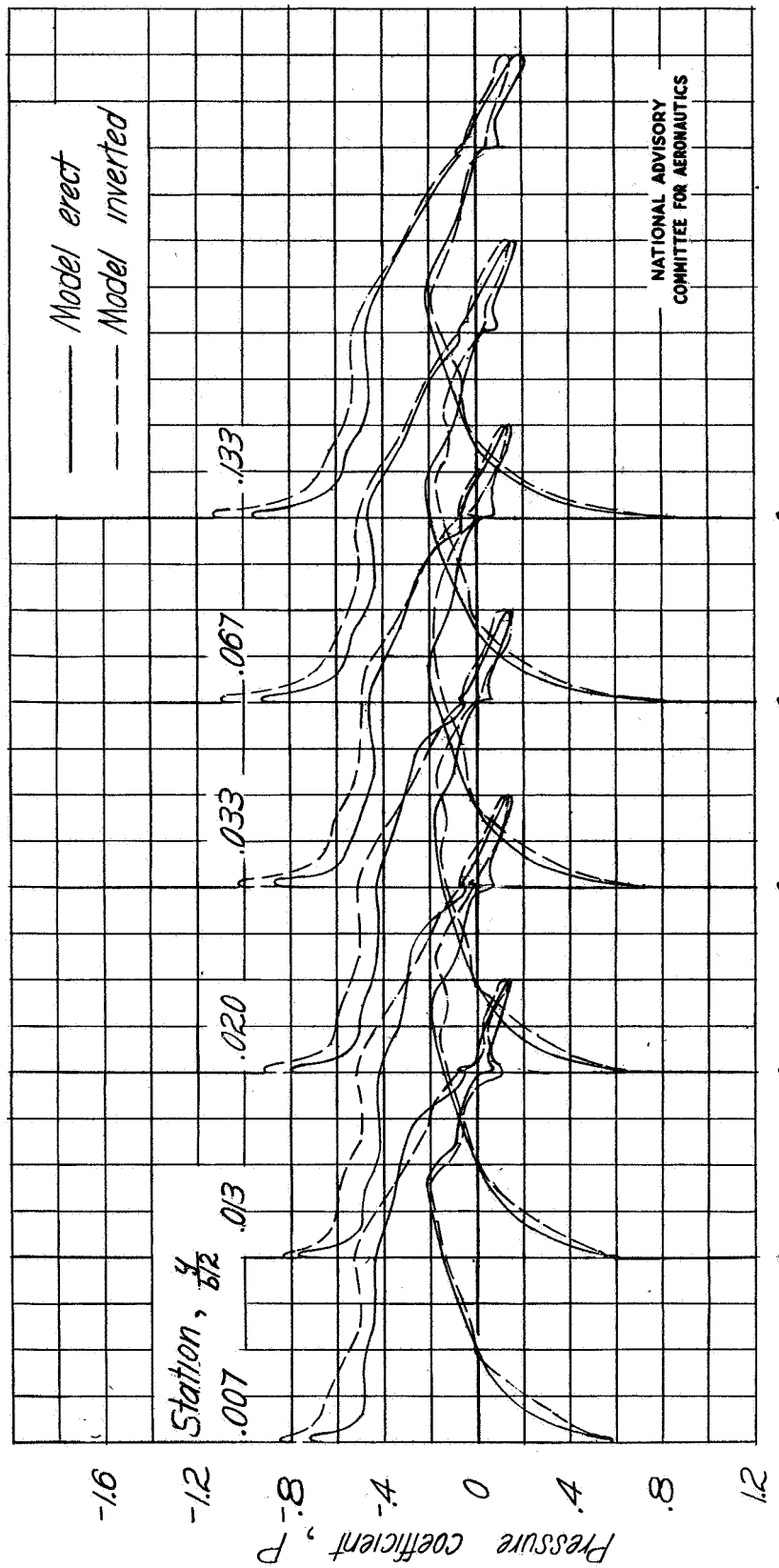

Figure 4.- Measured chordwise pressure distributions over a two-dimensional wing. Various spanwise tunnel positions; spoiler 2.

(a) $\alpha = 3.1°$; $R = 3.66 \times 10^6$.

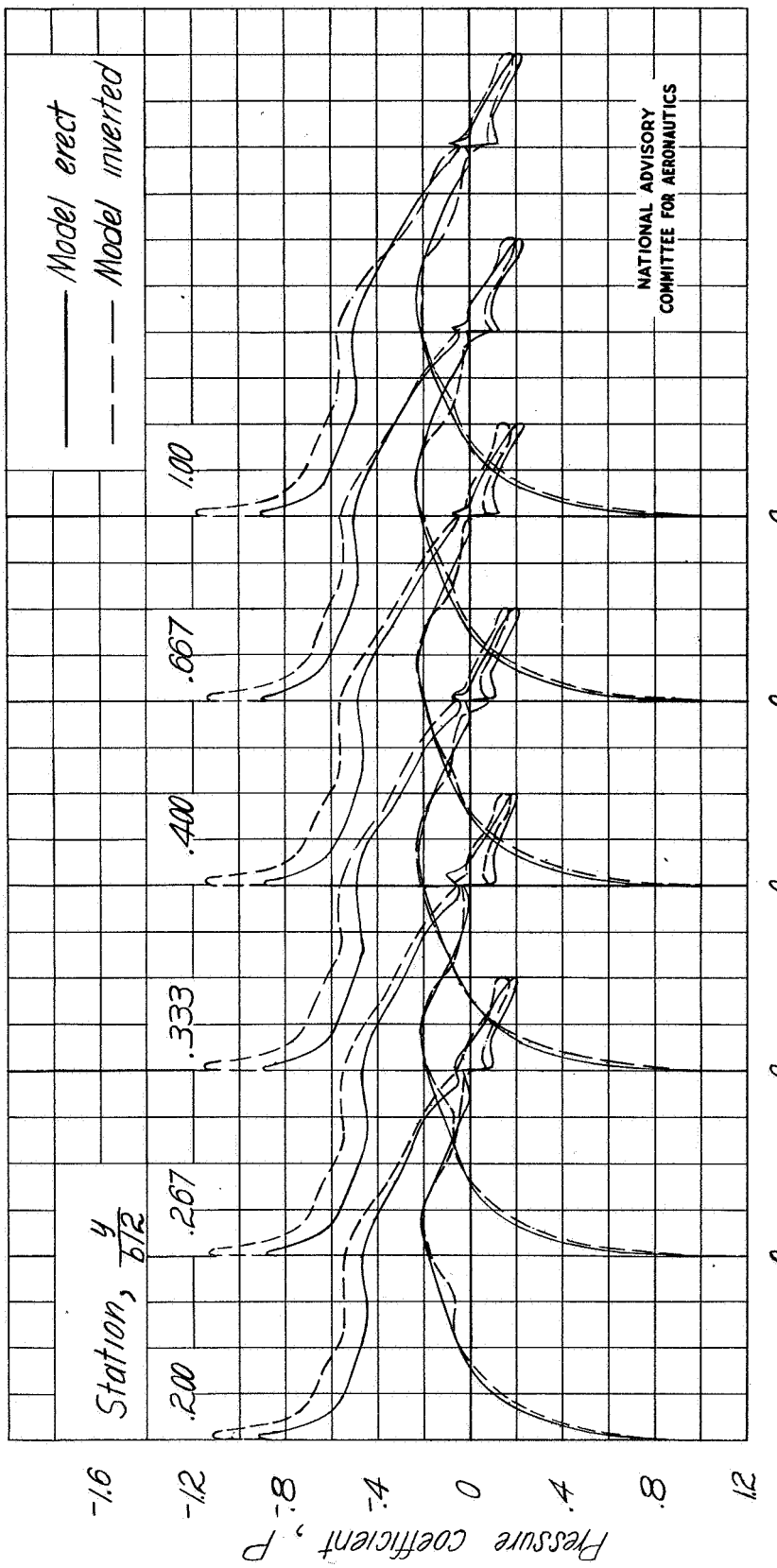

Figure 4.- Continued.

(a) Concluded.

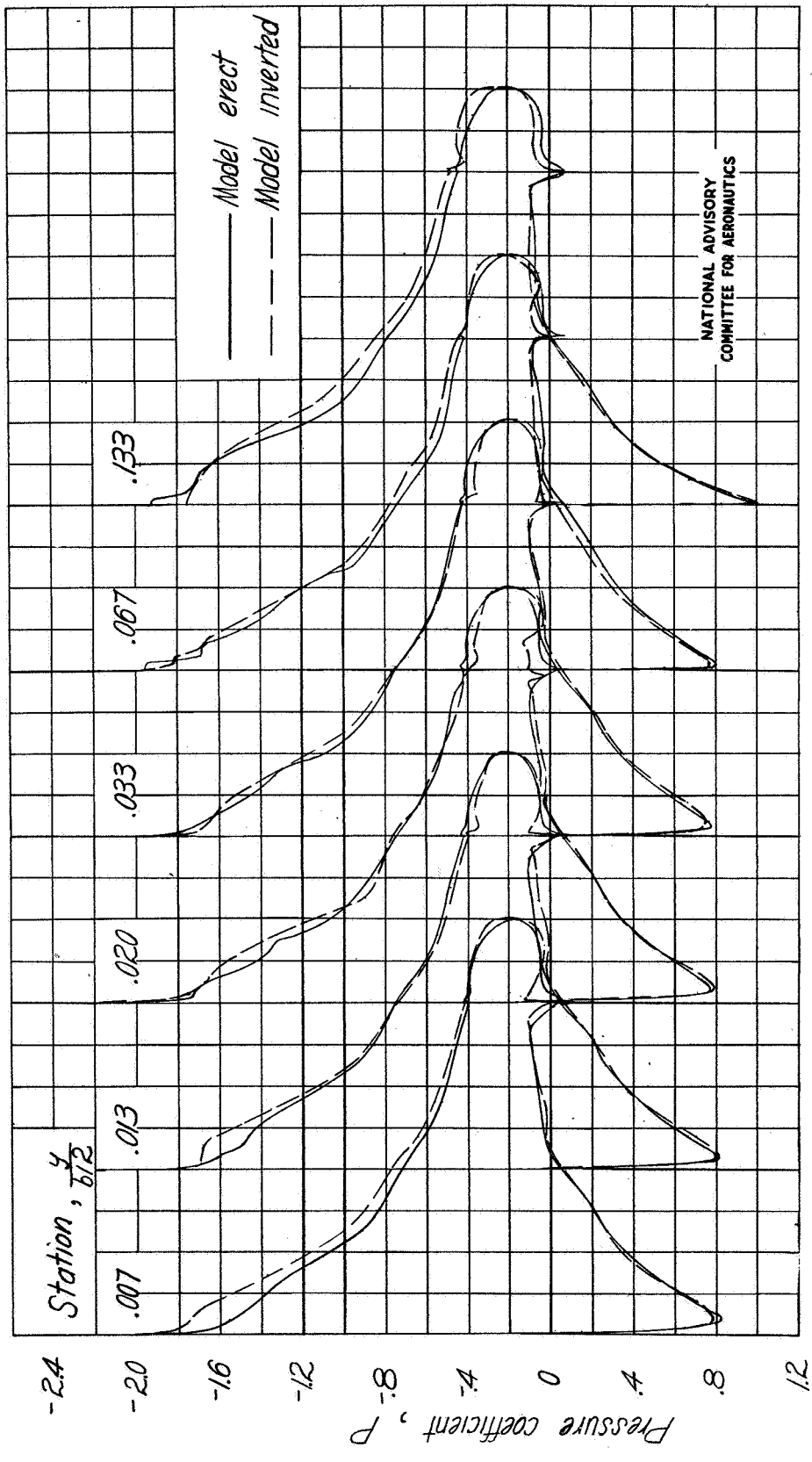

(b) $\alpha = 12.3°$; $R = 2.32 \times 10^6$.

Figure 4.- Continued.

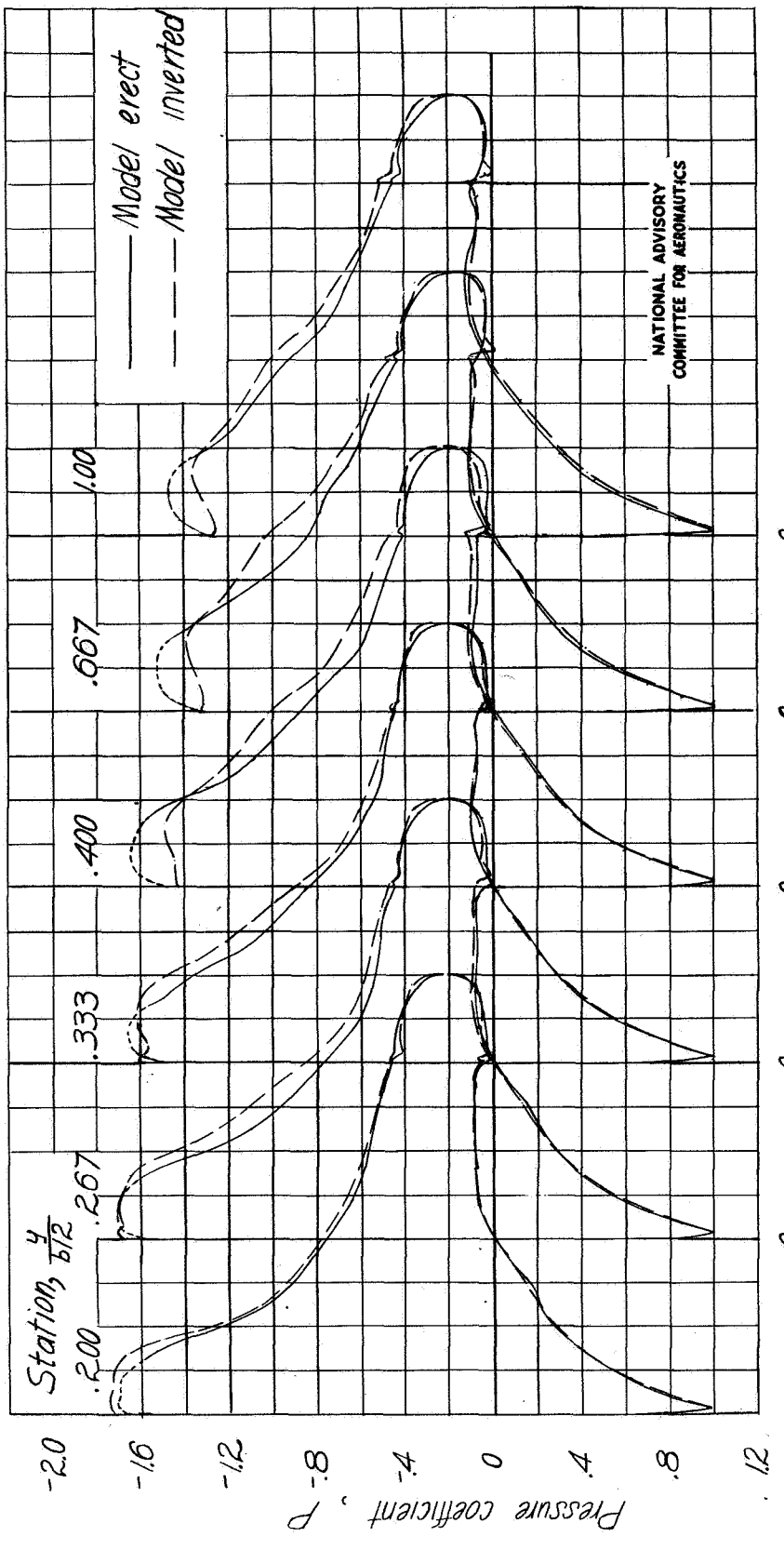

Figure 4.-Concluded.

(b) Concluded.

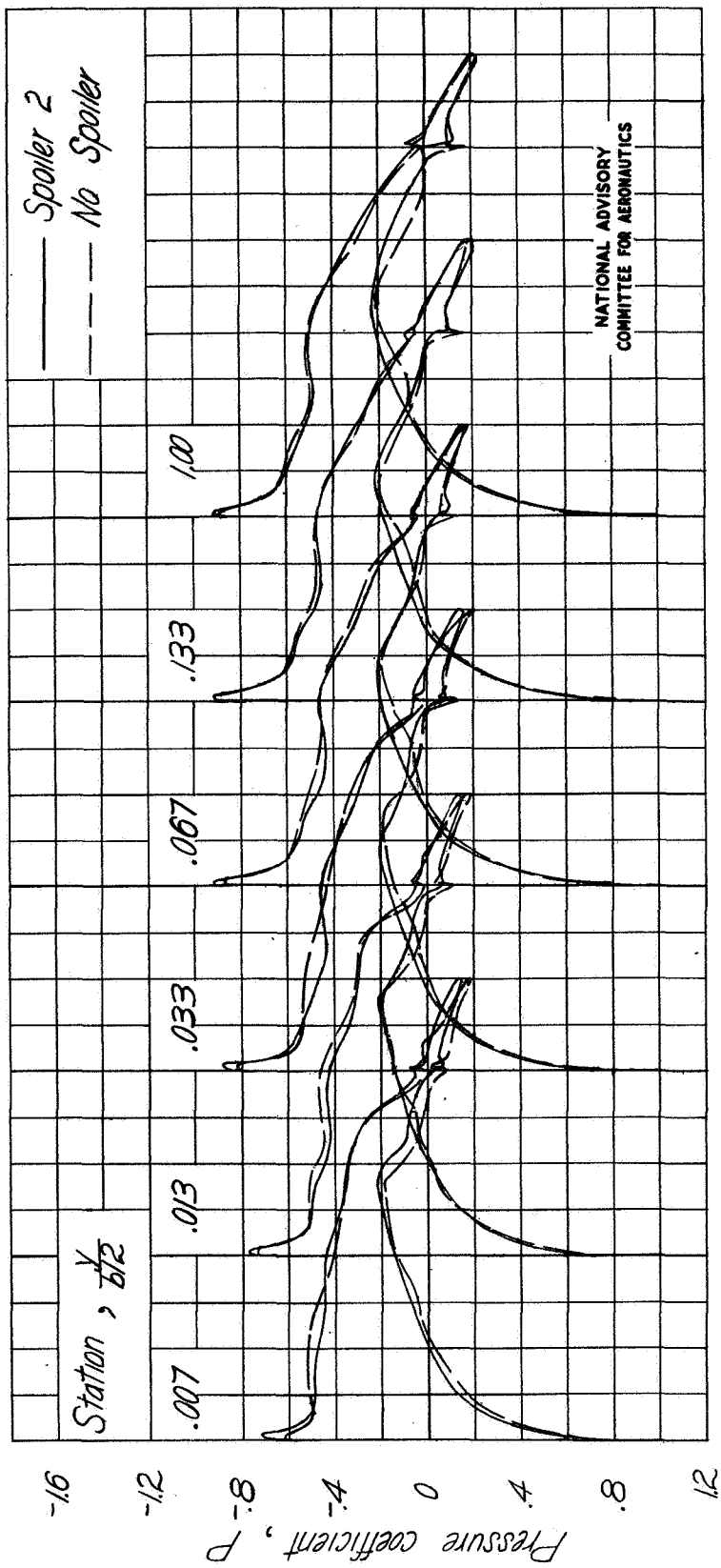

Figure 5.- Measured chordwise pressure distributions over a two-dimensional wing - Various spanwise tunnel positions, no spoiler and spoiler 2.

(a) $\alpha = 3.1°$; $R = 3.66 \times 10^6$.

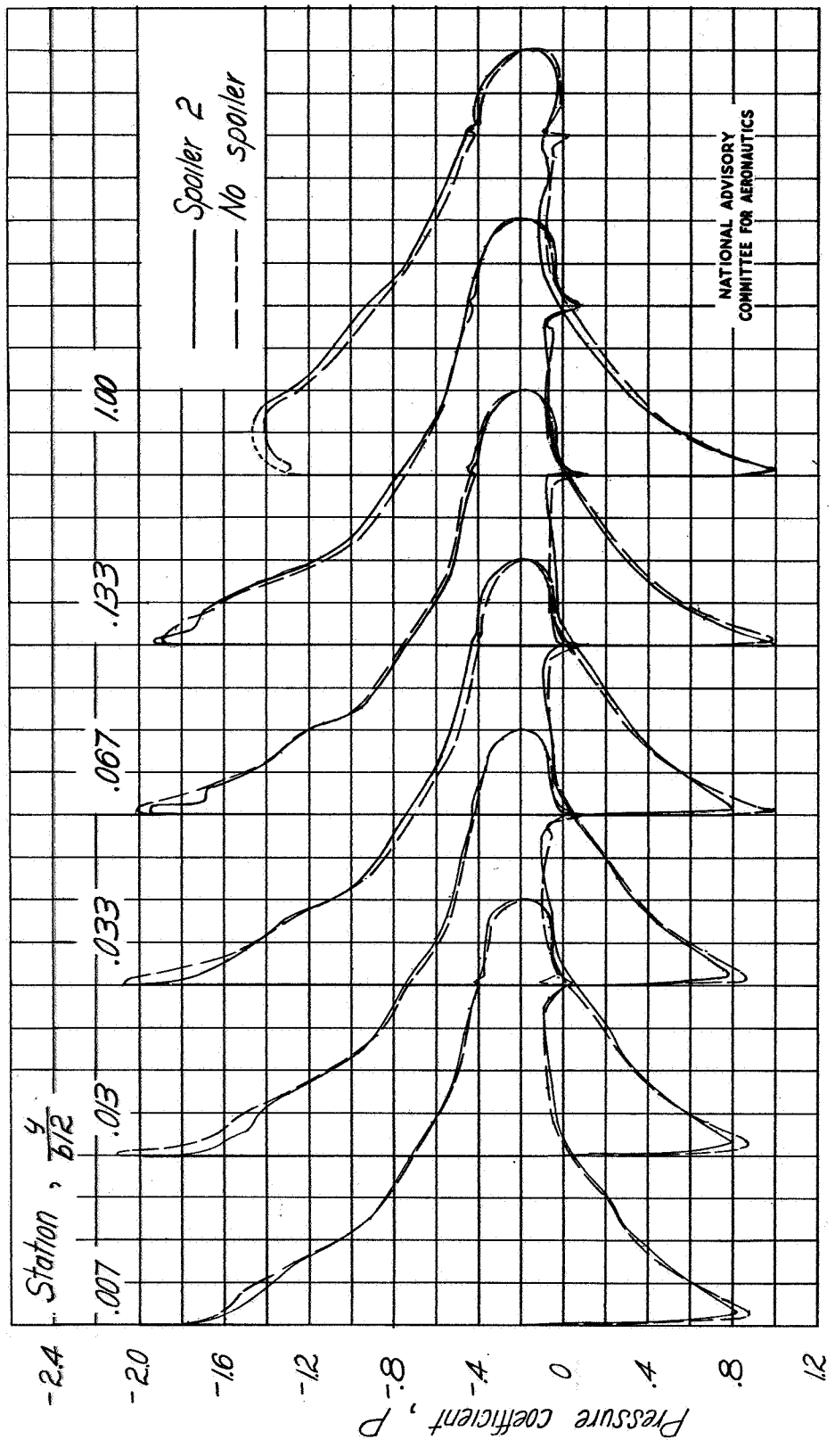

Figure 5.- Concluded.

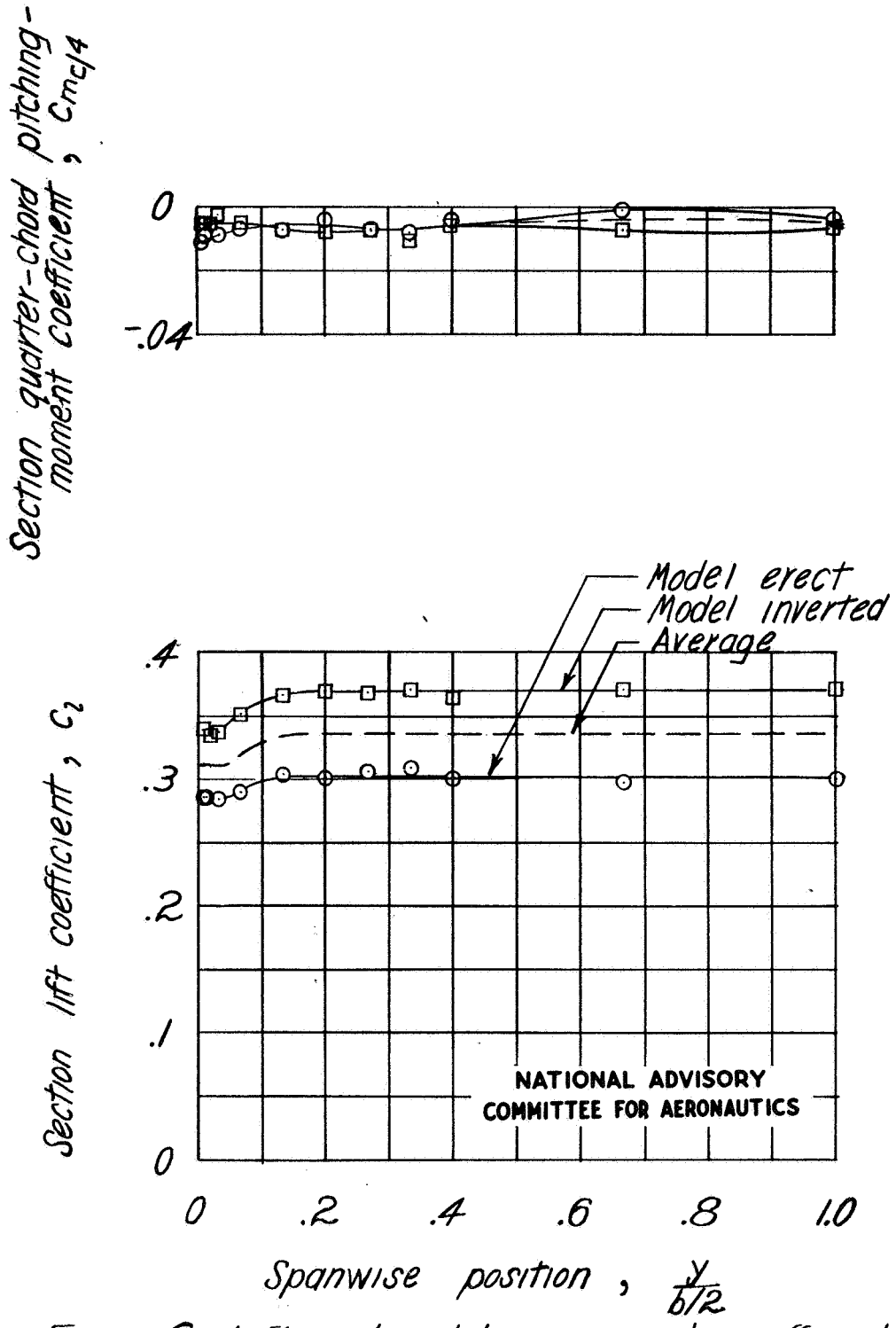

Figure 6.- Lift and pitching-moment coefficient curves for the erect and inverted model configuration, showing the method of averaging results. $\alpha = 3.1°$; spoiler 2; $R = 3.66 \times 10^6$.

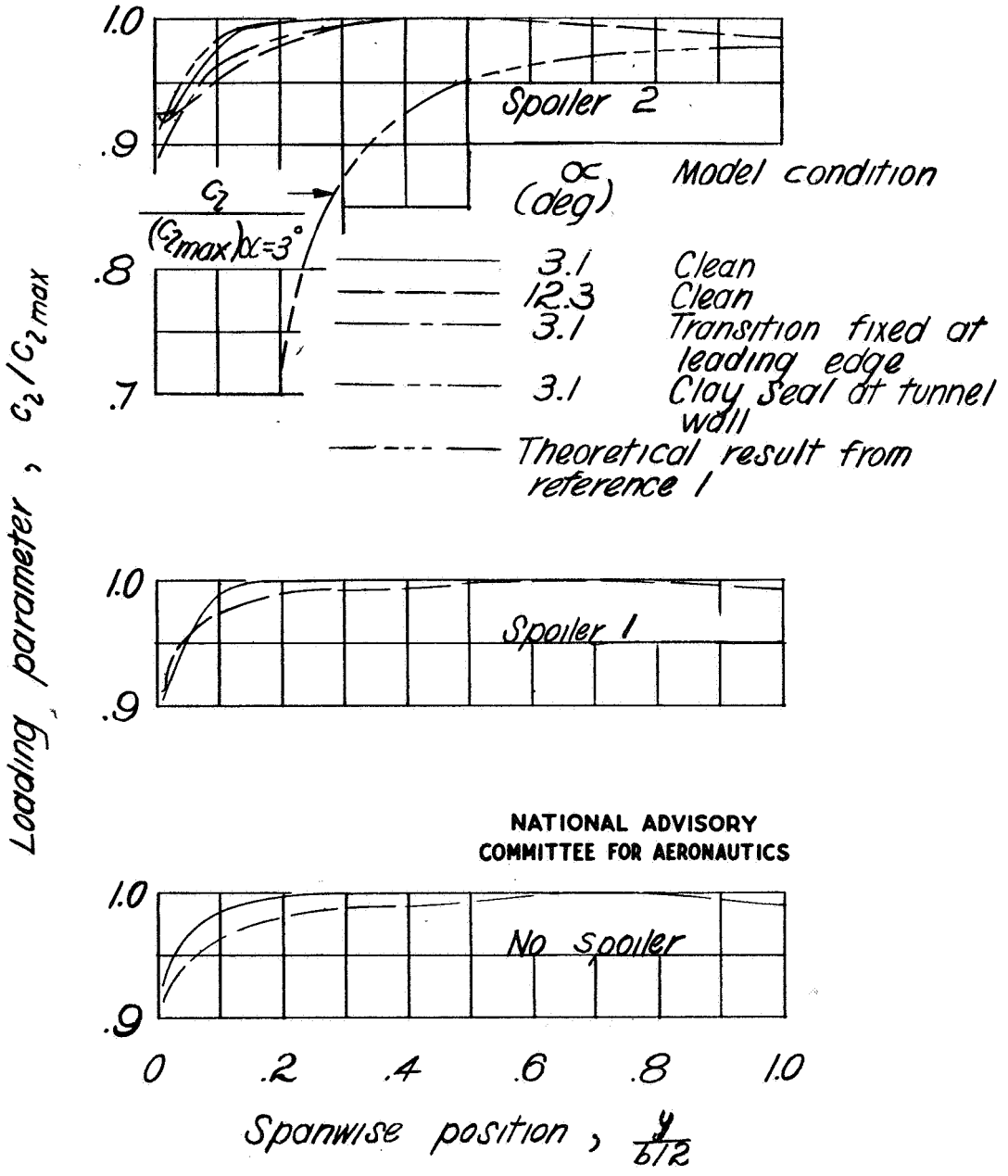

Figure 7.– Nondimensional span-loading curves for an NACA 65,-012 airfoil model completely spanning a tunnel test section. $R = 3.66 \times 10^6$ for $\alpha = 3.1°$ and $R = 2.32 \times 10^6$ for $\alpha = 12.3°$; average of erect and inverted model tests.

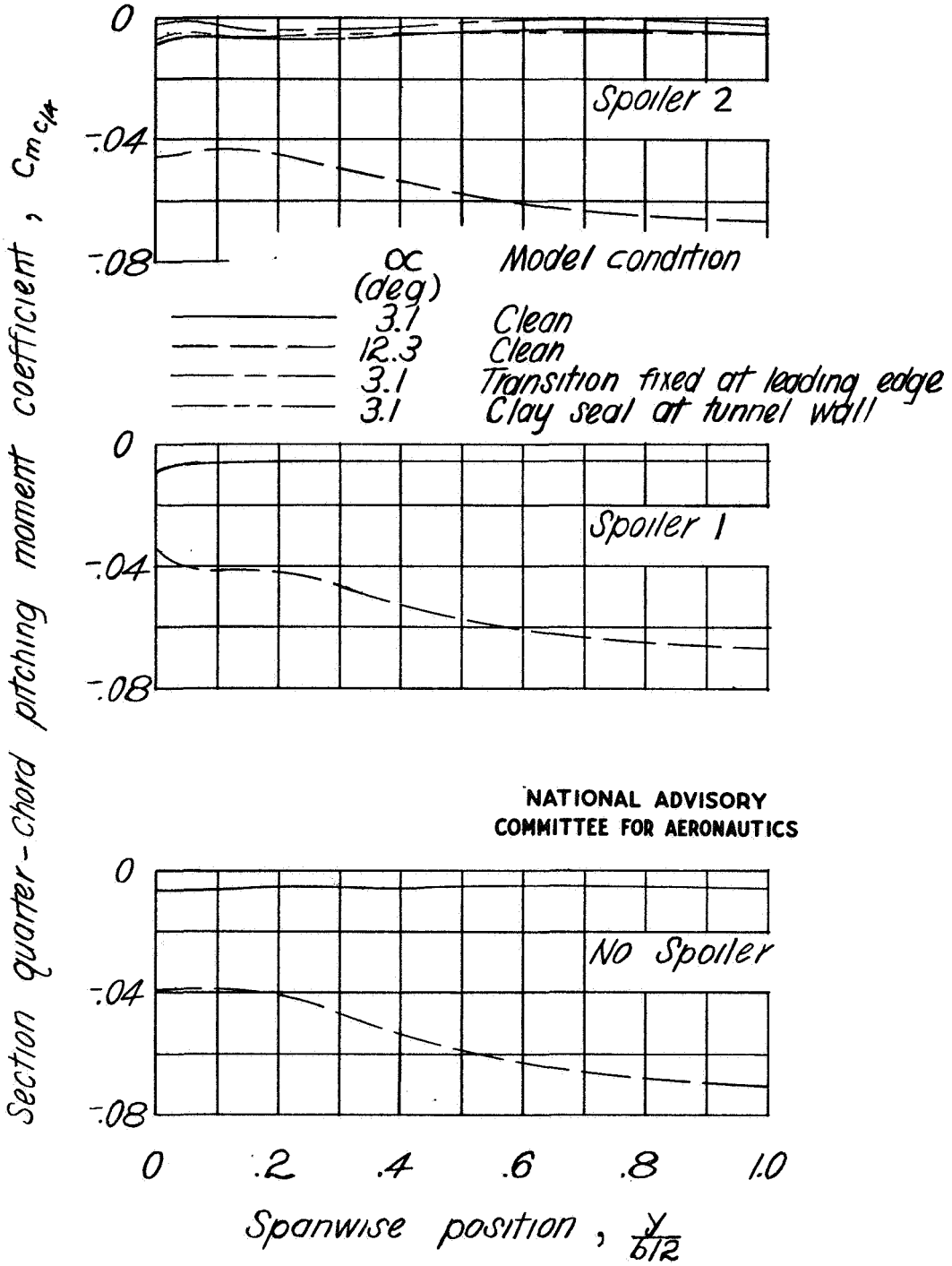

Figure 8.- Variation of section quarter-chord pitching-moment coefficient with spanwise position for an NACA 65,-012 airfoil model completely spanning a tunnel test section. $R = 3.66 \times 10^6$ for $\alpha = 3.1°$ and $R = 2.32 \times 10^6$ for $\alpha = 12.3°$; average of erect and inverted model tests.

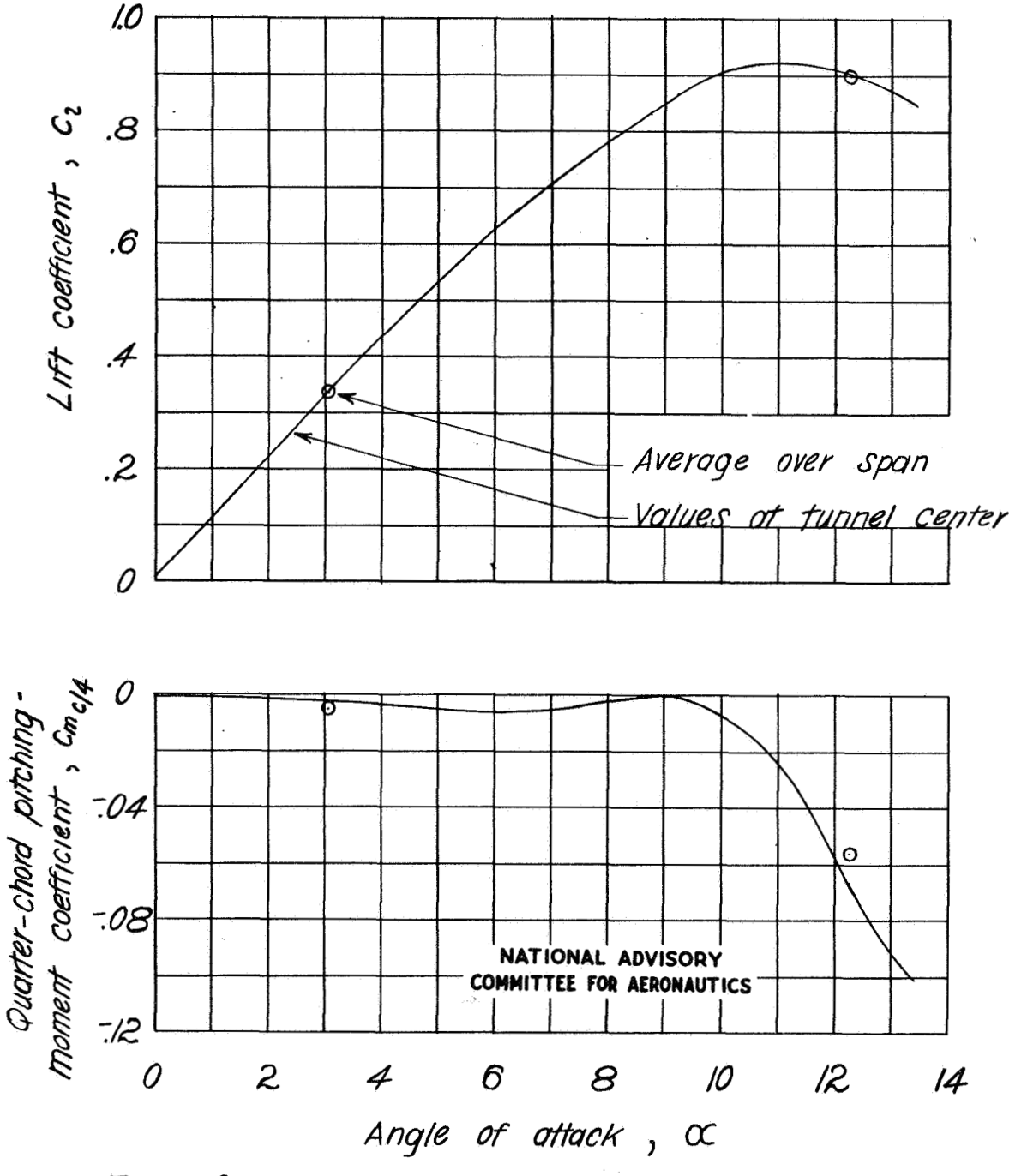

Figure 9.- Variation of C_L and $C_{m_{c/4}}$ with α for measurements at the center of the tunnel. $R = 2.32 \times 10^6$; average of erect- and inverted-model tests. Spoiler 2.